

# GRAVITY DRAINAGE KINETICS OF PAPERMAKING FIBROUS SUSPENSIONS

Piotr Przybysz<sup>1</sup>, Czesław Kuncewicz<sup>2\*</sup>, František Rieger<sup>3</sup>

<sup>1</sup>Lodz University of Technology, Institute of Papermaking and Printing, Wolczanska 229, 90-924 Lodz, Poland

<sup>2</sup>Lodz University of Technology, Faculty of Process and Environmental Engineering, Wolczanska 213, 90-924 Lodz, Poland

<sup>3</sup>Czech Technical University, Faculty of Mechanical Engineering, Technicka 4, 166 07 Prague, Czech Republic

The study analyses application possibilities of filtration and thickening models in evaluation of papermaking suspension drainage rate. The authors proposed their own method to estimate the drainage rate on the basis of an existing Ergun capillary model of liquid flow through a granular material. The proposed model was less sensitive to porosity changes than the Ergun model. An empirical verification proved robustness of the proposed approach. Taking into account discrepancies in the published data concerning how the drainage velocity of papermaking suspension is defined, this study examines which of the commonly applied models matches experimental results the best.

**Keywords:** drainage, fibrous suspensions, drainage kinetics

## 1. INTRODUCTION

The first stage in paper production on a paper machine is the formation of paper web from papermaking suspension. Generally the concentration of fibrous suspension fed to a paper machine ranges from 0.2-0.5%. This operation is carried out on a continuous moving wire in a forming section (commonly called a “wire” section) of a paper machine. During the forming process a paper web created on the wire is intensively drained. New high-speed paper machines need less than one second for this operation to be performed. In the first stage of drainage, water from the paper web is gravitationally removed with the use of static hydrofoils. As the wire with the wet web moves further, hydrofoils generate some vacuum that intensifies gravity drainage. When the paper web is drained up to 4-6% of fibrous suspension, a second drainage stage follows. In this stage, for further process intensification, suction boxes with vacuum are used. The final drainage element of the paper machine is a suction roll with two or three suction boxes. The final moisture content of the paper web after forming should be ca. 15-20% to obtain sufficient mechanical strength of a paper web so as to be safely transported to further sections of the paper machine.

Despite seemingly minor increase in suspension consistency during gravity drainage in the forming section, this is the paper machine section where the largest amount of water contained in the suspension is removed. In fact, around 85% of water flowing with the paper suspension to the paper machine is

\*Corresponding author, e-mail: [czeslaw.kuncewicz@p.lodz.pl](mailto:czeslaw.kuncewicz@p.lodz.pl)

[cpe.czasopisma.pan.pl](http://cpe.czasopisma.pan.pl); [degruyter.com/view/j/cpe](http://degruyter.com/view/j/cpe)

removed there. It means that in other parts, including the “dry end”, over five up to six times less water is removed than in the forming section alone. Since drainage in the forming section is less expensive than in other parts, tests on drainage kinetics and dynamics on the “wire” have some important practical implications. More information on processes during drainage can be found in Britt and Unbehend (1980); Ortner (2001); Smook (1992).

## 2. THEORY

A paper web is formed on the paper machine wire. Among other things, its structure depends on the properties of the papermaking suspension and the way it is formed. Although the general mechanism of this process is quite complex, when analysing it quantitatively, two basic mechanisms of fibrous suspension drainage on the wire are used, that is filtration and thickening. Both mechanisms were presented graphically in Wandelt et al. (2004).

In filtration mechanism, in drainage, successive layers of fibres and fines are settling down on the wire, increasing gradually the thickness of a paper web. This mechanism predominates in drainage processes with low dynamics at a relatively long dewatering time. The thickening mechanism is based on a constant increase in consistency in the total volume of drained suspension. This mechanism predominates in the processes with high dynamics making it difficult or even impossible for the sediment layer to be set on the wire.

Mathematical descriptions of the two mechanisms differ significantly. In case of the filtration mechanism the volumetric flow rate of received water (filtrate) is expressed by Eq. (1a, 1b) obtained from Ruth’s equation (Darby, 1996; Serwiński, 1982).

$$\dot{V} = \frac{dV}{d\tau} = A \cdot u = \frac{K}{2(V + C)} \quad (1a)$$

$$V^2 + 2VC = K\tau \quad (1b)$$

where  $V$  is the amount of removed water, and  $C$  and  $K$  are constants characteristic for a given suspension and filtration medium. Values of those constants are determined experimentally. In case of the thickening mechanism, the water flow through the suspension can be treated as a fluid flow through a granular layer with decreasing porosity  $\varepsilon$  in time. Smaller free spaces through which water flows also reduce the rate of water removed from the suspension being drained, but according to other relationships than those for the filtration mechanism. In case of the fluid flow through the granular layer two flow models can be considered, i.e. granular and capillary.

In the granular model (Serwiński, 1982), Leva equation (2) is valid. It combines a linear velocity of fluid flow  $u$  calculated for an empty apparatus with a generated driving force  $\Delta p$  that is the pressure difference above and under the layer

$$\Delta p = \lambda \left( \frac{h}{d_z} \right) \left( \frac{u^2}{2} \right) \rho_F \frac{(1 - \varepsilon)^2}{\varepsilon^3} \varphi^2 \quad (2)$$

where the drag coefficient  $\lambda$  and the Reynolds number  $Re$  for a laminar range of flow are expressed by Eq. (3)

$$\lambda = \frac{400}{Re} \quad Re = \frac{u d_z \rho_F}{\eta} \quad (3)$$

After substituting Eq. (3) into Eq. (2), Eq. (4) is obtained

$$\Delta p = \frac{200hu\eta}{d_z^2} \frac{(1-\varepsilon)^2}{\varepsilon^3} \varphi^2 \quad (4)$$

which shows that there is a direct proportional relationship between the fluid superficial velocity  $u$  and the driving force  $\Delta p$ .

In case of the capillary model of fluid flow through a granular layer, the layer alone is treated as a set of capillaries formed from intra granular free spaces linking the upper and the bottom surfaces of the bed. The basis of this model can be found in the earlier fundamental papers (Blake, 1922; Carman, 1937; Kozeny, 1927). Not going into derivation details, the authors obtained Eq. (5), where the drag coefficient  $\lambda$  and the Reynolds number are defined by Eqs. (6) and (7).

$$\Delta p = \lambda_E \left( \frac{1-\varepsilon}{\varepsilon^3} \right) u^2 \rho_F \left( \frac{h}{d_z} \right) \quad (5)$$

$$\lambda_E = \frac{a_E}{Re} \quad (6)$$

$$Re = \frac{ud_z \rho_F}{(1-\varepsilon)\eta} \quad (7)$$

The constant  $a_E$  in Eq. (6) characterises resistance of the liquid flow through free spaces of the granular layer. The literature review shows that even for the laminar regime ( $Re < 10$ ) there is no consensus regarding its value. Suggested values usually range from 150 to 200. However the most frequently used values are those determined by Carman (1937)  $a_E = 180$  or  $a_E = 150$  determined by Ergun (1952). Despite numerous experiments carried out by researchers, there is no agreed constant value  $a_E$ . This is mainly due to a huge number of possible granule shapes. For example, granules may be similar to spheres or, as in the case of papermaking suspension, they may be non-isometric. In such a case, only forms of Eqs. (5-6), without a specific constant value  $a_E$ , may be used. Equation (5) is known as Blake-Kozeny-Carman equation or Ergun equation, depending on the constant value of  $a_E$  used.

Regardless of the numerical constant value of  $a_E$ , after combining Eqs. (5), (6) and (7), Eq. (8) can be obtained, which also indicates a direct proportionality between the driving force and the superficial velocity of the removed water,  $u$ .

$$\Delta p = a_E \left( \frac{hu\eta}{d_z^2} \right) \frac{(1-\varepsilon)^2}{\varepsilon^3} \quad (8)$$

When comparing Eqs. (4) and (8) derived from two different models of the liquid flowing through a granular layer in the laminar regime (thickening of papermaking suspension), it is easy to notice how similar they are. The equations differ only in the values of constants and in an additional parameter  $\varphi$  occurring in the Leva equation (2). It should be stressed, however, that both equations describe resistance of liquid flow through a fixed granular layer with parameters fixed in time.

It is difficult to find papers in scientific literature that explicitly show which of the three presented models (filtration model or two models of flow through a granular layer) describes better kinetics of fibrous suspension drainage on the wire in the forming section of the papermaking machine. Apart from that, results included in the available papers are quite equivocal. For example, in the paper of Parker (1992) sheet formation on the paper machine wire was analysed as a two-stage process. In the first stage, when the suspension consistency is low and the suspended fibres still to some extent move freely, drainage takes place in accordance to the filtration model. When fibres are immobilised in the already partly thickened structure, further drainage is performed according to the thickening mechanism. The drainage process is treated slightly differently in other papers (Cole at al., 2008;

Hubbe et al., 2008). According to results provided there, the thickening mechanism differs from that of the filtration mechanism, and the fine content is a criterion deciding which of the two eventually prevails. If the fine content is less than 30%, the filtration mechanism dominates in the drainage process. Recent experiments (Wandelt and Perlińska-Sipa, 2007; Wandelt and Perlińska-Sipa, 2008) on static and dynamic drainage were carried out in a vertical cylinder with a wire bottom being a model of a wire in the paper machine forming section. In both cases gravitational water flow through the wire bottom occurred, but in the dynamic process a high-speed agitator working right above the bottom was additionally used. It was found, that in the static process, the filtration mechanism predominated, whereas in the dynamic dewatering it was the thickening mechanism. To describe the filtration mechanism, the authors (Wandelt and Perlińska-Sipa, 2007; Wandelt and Perlińska-Sipa, 2008) used the classic Ruth's equations (1a, 1b) derived for a constant filtration driving force. However, in this case, the equations may have limited application, as the driving force (height of a suspension column) changes with time. Apart from that, in the paper of Wandelt and Perlińska-Sipa (2007) data obtained from the model were not compared with experimental results.

As regards predominance of one of the mechanisms, different conclusions can be drawn from the analysis of the work by Britt et al. (1986). Laboratory tests found that with a fast drainage on high-speed paper machines, the main drainage process is accomplished according to the thickening model. Only in a few cases with very slow drainage a partial filtration of papermaking suspension can follow.

Taking into account a very short time of suspension drainage on the wire lasting just a fraction of a second, it can be assumed, that such time is too short for the papermaking suspension to settle on the wire. Thus the thickening mechanism is more likely to be expected. However, when trying to develop a new mathematical description of the thickening process, a peculiarity of the water flow during suspension drainage has to be considered. During the drainage process, the papermaking suspension does not gradually settle down on the wire but it is progressively thickening in its entire volume. Therefore, according to Eq. (8), in order to be removed from the suspension to a container under the wire, water has to flow through free spaces of the suspension (decreasing with time) with a velocity  $u_0$  higher than that following from Eq. (9)

$$u_0 = \frac{u}{\varepsilon} \quad (9)$$

The mechanism presented above was the starting point for our own drainage model, in fact, being a modification of granular models. In general, it was decided to base the model on the existing Blake-Kozeny-Carman or Ergun Eq. (8). A modification was mainly performed by using a different definition of the Reynolds number than that for the filtration model and both thickening models. It was assumed that the character of the water flow through thickening suspension should be influenced by the current velocity  $u_0$ , i.e. the velocity of the water flow between the fibres. Considering the fact that the porosity of the drained pulp is very high, amounting to  $\varepsilon = 0.9$  or more, the relative movement of the liquid and the fibers may be regarded as disrupted descent of the solid (fibers) in a liquid. Then the definition of the Reynolds number will be expressed by Eq. (10). Having combined Eqs. (5), (6), (9) and (10), we will obtain Eq. (11) defining the resistance of the water flow  $\Delta p$  through the thickening suspension.

$$Re = \frac{u_0 d_z \rho_F}{\eta} \quad (10)$$

$$\Delta p = a_E \left( \frac{h\eta}{d_z^2} \right) \left( \frac{1-\varepsilon}{\varepsilon^2} \right) u \quad (11)$$

Equation (11) differs from the classic Ergun relationship (8) by terms containing porosity  $\varepsilon$ . As mentioned before, it is a consequence of a different definition of the Reynolds number. Despite some similarities between Eqs. (8) and (11), the numerical values  $\Delta p$  for fixed velocity  $u$  (or value  $u$  for fixed

$\Delta p$ ) may vary even several times. Apart from that, in the case of suspension drainage on the paper machine wire, the value of  $\varepsilon$  changes with time.

It should be noticed, that Eq. (11) was derived including an intuitional assumption regarding characteristic dimension  $d_z$  and velocity  $u_0$  in the definition of the Reynolds number (Eq. (10)). Due to the lack of theoretical background for such an assumption, Eq. (11) has to be verified experimentally.

### 3. EXPERIMENTAL

In order to determine experimentally the rate of suspension drainage the testing equipment presented in Fig. 2 was constructed (Przybysz et al., 2014).

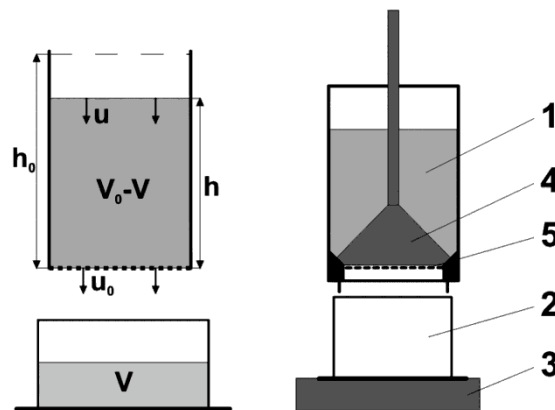


Fig. 1. Simplified scheme of testing equipment

The main element of the equipment was a measuring cylinder (1) with a diameter of 100 mm and height 140 mm, containing about 1000 ml of suspension of different concentrations  $c_0$ . Below the cylinder there was a container (2) for water removed from the suspension and an electronic scale (3) (measurement accuracy of 0.1 g) to weigh the amount of removed water with a frequency of 20 readings per second. The time  $\tau$  [s] and the water weight  $m$  [kg] were recorded on-line by a computer (not illustrated in the figure). Additionally, a sealing cone (4) was installed in the container that, when lifted, allowed water to flow through the suspension and the wire screen (5). Based on the measurements, a drainage curve was plotted as a sequence of experimental points  $m = f(\tau)$ .

#### 3.1. Determination of flow parameters variables

Having measured weight  $m$  of water that was withdrawn from the bottom wire screen for particular times  $\tau$  it was easy to determine a mass fraction and a volume fraction  $x$  of water flowing out to the space under the wire screen and hence to calculate the current height  $h$  of the suspension in the cylinder. Due to a very low initial concentration of the papermaking suspensions ranging from 0.08 to 0.32% and the density of dry pulp ( $\rho \sim 1500 \text{ kg/m}^3$ ), it can be assumed that the density of the suspension during the whole experiment was invariable and equal to  $\rho_F = 1000 \text{ kg/m}^3$ . In the tests, the authors used a suspension prepared from unbleached pine kraft pulp. The pulp was delivered by a paper mill in the form of air-dried sheets. The initial freeness value of the pulp was  $13^\circ \text{SR}$ .

When analysing the results of experimental measurements it had to be considered that the experiments were conducted as an unsteady-state process and three main process parameters – the velocity of lowering liquid level  $u$ , suspension porosity  $\varepsilon$  and driving force  $\Delta p$  - were varied with time and they had to be initially determined based on the drainage curve  $m = f(\tau)$ .

### 3.2. Velocity of liquid flow

In the easiest way, transient velocity of the lowering liquid level  $u$  in the cylinder could be calculated as a ratio of an increase in weight of water collected under the wire (its volume) to time intervals. Unfortunately, the time intervals were very small, ca. 0.05 s, and the increase in water weight was within an experimental error of determining this parameter. Therefore, it was decided to determine value  $u$  based on the approximation of an experimental relationship  $x = f(\tau)$  using a mathematical formula and then its differentiation in order to obtain the searched velocity value. In the laminar regime (in the discussed case, the liquid flow in the bottom openings was laminar), the water flow velocity is proportional to the transient driving force i.e. corresponding to the first order process kinetics. The solution of this problem is Eq. (12), where constant  $k$  [1/s] is a characteristic velocity constant of the process.

$$x = \frac{V}{V_0} = 1 - \exp(-k\tau) \rightarrow V = V_0 \cdot [1 - \exp(-k\tau)] \quad (12)$$

Equation (12) refers to the case when the velocity constant  $k$ , being an inverse of flow resistance, has an invariable value and then we should obtain a straight line in the coordinates  $\ln(1-x) = f(\tau)$ .

Figure 2 shows results obtained for the papermaking suspension with 13°SR value for four initial pulp concentrations  $c_0 = 0.08, 0.16, 0.24$  and  $0.32\%$ . As presented in Fig. 2, in all the cases it can be assumed that the points are located along straight lines despite the fact that always at the beginning of the flow, experimental points are placed slightly below the straight line (the actual flow was faster than that resulting from the first order model), whereas for long times the flow was significantly decreasing as the water was only dripping from a formed layer of the papermaking web. However, the majority of the experimental points were located along a straight line. The figure also shows the values of rate constants  $k$  calculated from Eq. (12). As expected, the higher was the concentration of the suspension, the lower was its porosity, and the rate constant had lower values. Similar diagrams and a similar agreement were also found for other papermaking suspension freeness of 13, 19, 32 and 36 °SR.

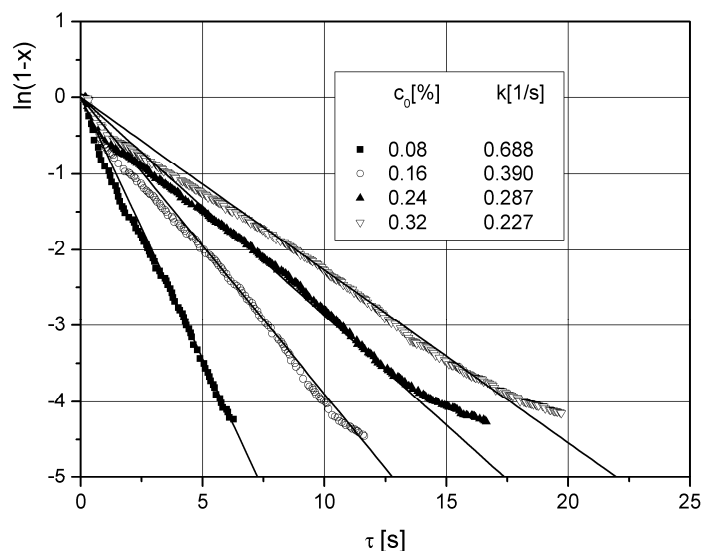


Fig. 2. Verification of compatibility of water flow velocity with model of first order process

On the other hand, a temporary velocity of the water level lowering  $u$  in the cylinder can be defined by Eq. (13). Including relationship (12) in it, we can obtain Eq. (14) determining a value of  $u$  necessary for further calculations.

$$u = \frac{dV}{Ad\tau} \quad (13)$$

$$u = \frac{V_0}{A} \cdot k \cdot \exp(-k\tau) \quad (14)$$

Figure 3 illustrates experimental points and a line obtained from Eq. (12) for gravity drainage of 13°SR suspension. To make the figure more transparent, it contains only one line for the suspension with the initial suspension concentration  $c_0 = 0.08\%$ . As seen in Fig. 3, the function (12) fits well the experimental points. The figure also shows the velocity  $u$  calculated from Eq. (14). Its value is proportional to a slope of tangent to the curve  $x = f(\tau)$ . The velocity was changing from the maximum value  $u = 0.032$  m/s at the beginning of the drainage process (at  $\tau = 0$ ) to a value about hundred times lower at the end of it. The average value, calculated from Eq. (13) based on experimental global values  $\Delta V$ ,  $\Delta\tau$  and surface  $A$ , was 0.007 m/s and was four and a half times lower than the maximum velocity.

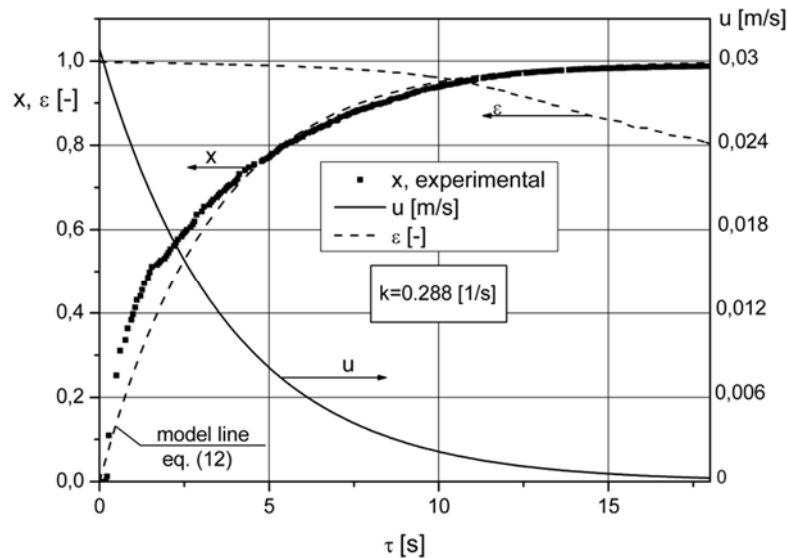


Fig. 3. Gravity drainage of suspension with 13°SR value and initial concentration  $c_0=0.08\%$

### 3.3. Porosity of drained suspension

Porosity plays a key role in the resistance of water flow during suspension drainage. This results from analysis of Eq. (11). In particular, significant changes are connected with an alteration of the term  $(1-\varepsilon)$ , which at the beginning was equal to 0.002–0.005 and at the end of drainage reached values in the range of 0.1–0.2. A current value of  $\varepsilon$  can be determined by performing the mass balance of a solid and by bearing in mind that the mass of a solid remains constant with time. After simple transformations, Eq. (15) can be obtained, where  $\varepsilon_0$  means porosity at  $\tau = 0$  and its value can be calculated if the initial suspension concentration  $c_0$  is known.

$$\varepsilon = 1 - \frac{1 - \varepsilon_0}{1 - x} \quad (15)$$

Figure 3 shows the porosity  $\varepsilon$  of the suspension changing with time calculated from Eq. (15) (dashed line). At the beginning of drainage, suspension porosity was close to unity, while at the end it approached the value of 0.8.

### 3.4. Driving force in gravity drainage

Hydrostatic pressure of liquid above the wire is a driving force for gravity drainage:  $\Delta p = h \cdot \rho_F \cdot g$ . However, the driving force causes not only liquid flow through a suspension but it has to overcome the

resistance of the flow through the wire bottom. Therefore, the actual drainage driving force  $\Delta p_{\text{sus}}$  of gravity drainage is a difference between the entire driving force  $\Delta p$  and resistance  $\Delta p_{\text{bot}}$  of the flow through the bottom.

$$\Delta p_{\text{sus}} = \Delta p - \Delta p_{\text{bot}} \quad (16)$$

The resistance of the bottom wire screen can be calculated on the basis of our previous paper (Przybysz et al., 2014) where the problem of the bottom wire screen resistance was analysed in detail. The calculations show the resistance is approximately equal to 15% of the overall flow resistance during drainage and is also a function of the flow velocity  $u$ . Thus, the driving force  $\Delta p_{\text{sus}}$  can be expressed as follows

$$\Delta p_{\text{sus}} = \Delta p - \Delta p_{\text{bot}} \quad (17)$$

Where the value  $h_{\text{bot}}$  was determined in our previous paper (Przybysz et al., 2014)

#### 4. ANALYSIS OF THE OBTAINED RESULTS

The purpose of the study was to determine the mechanism of papermaking suspension gravity drainage. In case of filtration mechanism, Eq. (1a) is valid and can be transformed to

$$\frac{K}{u} = 2A (V + C) \quad (18)$$

The value of the filtration constant  $K$  in Eq. (18) is directly proportional to the driving force (Serwiński, 1982). Since in our tests  $\Delta p = (h - h_{\text{bot}}) \cdot \rho_F \cdot g$ , it means that  $K \propto (h - h_{\text{bot}})$ . Additionally, taking into account that the amount of water collected under the wire  $V \propto x$ , after simple transformations Eq. (19) can be obtained

$$\frac{h - h_{\text{bot}}}{u} = k_1 \cdot x + k_2 \quad (19)$$

Where the value  $k_1$  and  $k_2$  are constant. It means that experimental points in the co-ordinate system  $(h - h_{\text{bot}})/u = f(x)$  should be positioned along a straight line.

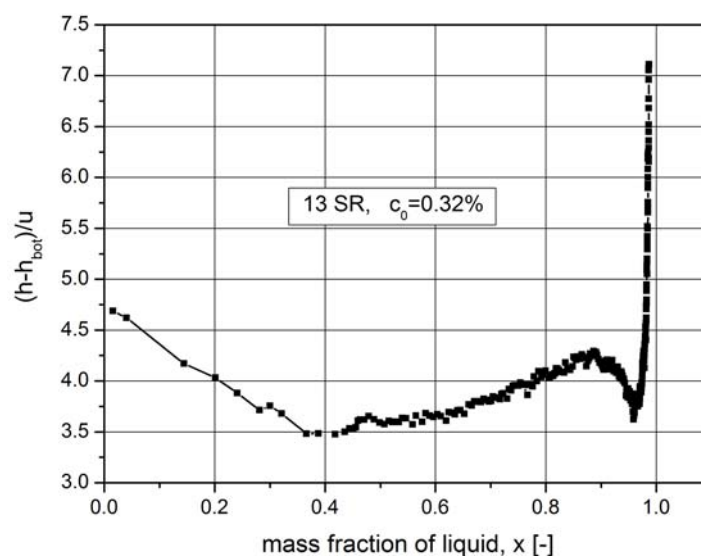


Fig. 4. Verification of filtration model



Figure 4 presents an experimental verification of the filtration model. It shows the relationship (19), where all the parameters change with time ( $u$ ,  $\varepsilon$  and  $\Delta p$ ). They were determined according to the methodology presented in the previous section. As Fig. 4 shows, the derived filtration model is not in agreement with the experimental results. The experimental data points are scattered along an irregular curve with a clear vertical asymptote. The lack of a straight line in Fig. 4, i.e. no agreement between the filtration model and the experimental data is most likely resulting from a too short drainage process. The suspension had not sufficient time to be deposited on the wire medium. The curves, similar to those in Fig. 4, were also obtained for the papermaking suspensions of different freeness values [°SR].

In the case of mechanisms based on the liquid flow through granular layers (the granular and capillary models) the literature contains relationships similar (4) and (8). These are Leva and Ergun equations that differ only in constants and the shape factor  $\varphi$  of a single fiber invariable for a given suspension. It means that both models can be verified with a single calculation procedure. For example, introducing Eq. (17) to Ergun equation (8), after simple transformations we obtain

$$u = \frac{d_z^2}{a_E} \cdot \frac{\rho g}{\eta} \cdot \left( \frac{h - h_{\text{bot}}}{h} \right) \cdot \frac{\varepsilon^3}{(1 - \varepsilon)^2} \quad (20)$$

which means, that if the model was valid, the experimental points in the co-ordinates  $u$  and  $\left( \frac{h - h_{\text{bot}}}{h} \right) \cdot \frac{\varepsilon^3}{(1 - \varepsilon)^2}$  should provide a straight line passing through the origin of the co-ordinate system.

Figure 5 shows the results of experiments in the co-ordinate system defined by Eq. (20). As Fig. 5 indicates, the experimental points collected in each experimental pass through the origin of the co-ordinate system, although they are not located along straight lines. It means that the results of the experiments do not fulfill the requirements of any model of the liquid flow through granular layers following from Eq. (4) and Eq. (8).

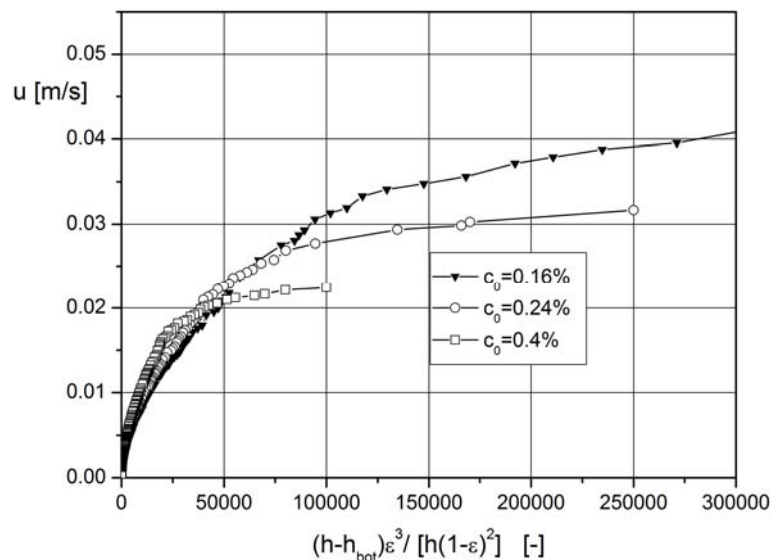


Fig. 5. Verification of granular models

The final stage of the study was to check the correctness of the authors' own model of the papermaking suspension thickening suggested in Eq. (11). The model is a modification of the existing granular models.

Starting with Eq. (11) and including the resistance of flow through the wire bottom defined with Eq. (17) we obtain

$$u = \frac{d_z^2}{a_E} \cdot \frac{\rho g}{\eta} \cdot \left( \frac{h - h_{\text{bot}}}{h} \right) \cdot \frac{\varepsilon^2}{1 - \varepsilon} = B \cdot \left( \frac{h - h_{\text{bot}}}{h} \right) \cdot \frac{\varepsilon^2}{1 - \varepsilon} \quad (21)$$

It can be noticed easily, that Eq. (21) differs from Eq. (20) only by having lower values of the exponents at  $\varepsilon$  and  $(1-\varepsilon)$ .

Figure 6 shows a verification of the authors' own gravity drainage model in the co-ordinate system resulting from Eq. (21). The experimental points for the papermaking suspension of 13°SR were positioned along the same straight line, for all five tested initial concentrations  $c_0$  of the papermaking pulp. The obtained straight line proves that the relationship (21), derived from the Ergun equation, well describes the behaviour of the papermaking suspension during the drainage process. A common value of the slope of the straight line equals to  $8.84 \times 10^{-5} \text{m/s}$  and results from the fact that, according to Eq. (21), the value of the constant  $B$  should not depend on the initial pulp concentration, as all the values on the left side of Eq. (21) do not depend on this parameter.

$$\frac{d_z^2}{a_E} \cdot \frac{\rho g}{\eta} = B = 8.84 \times 10^{-5} \text{ [m/s]} \quad (22)$$

Unfortunately, we are not able to determine from Eq. (22) either a value of  $d_z$  for a single fibrous suspension or a value of  $a_E$ , except for their ratio  $d_z^2 / a_E$ . For the papermaking pulp of freeness 13°SR, it is  $8.98 \times 10^{-11} \text{m}^2$ .

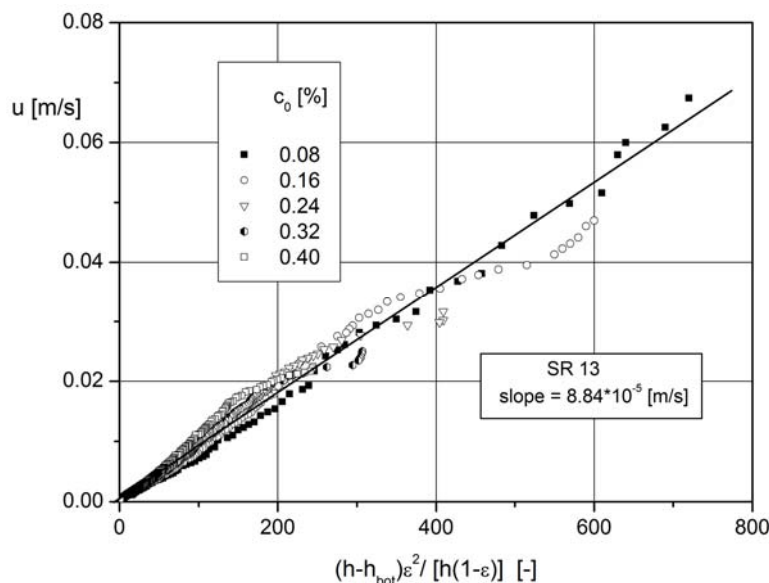


Fig. 6. Verification of model based on Eqs. (11) and (21)

A low value of the ratio  $d_z^2 / a_E$  results mainly from a low value of the equivalent diameter  $d_z$ . It should be noticed that the method for porosity determination, accepted in this study, did not include water inside cellulose fibres increasing in this way their size and therefore the size of the equivalent diameter  $d_z$ . The equivalent fibre diameter in the proposed model includes only dry fibres in the suspension. To determine the value of  $d_z$  we cannot use a constant value of  $a_E$  determined by Carman (1937), which equals 180 or a value of  $a_E = 150$  determined by Ergun (1952) due to a different definition of Reynolds number and due to the fact that the papermaking suspension contains non-isometric particles.

A value of the constant  $B$  should depend on the suspension freeness value, as during a refining process with a very high shear rate and high shear stress in the refiner, cellulose fibres become elastic and partly fragmented. It should make fibres more tightly arranged in the paper web, thus reducing free spaces where water can flow through. As a result, the flow resistance should increase. In addition, the

size reduction of fibres should result in a smaller equivalent diameter  $d_z$  followed by an increased flow resistance and decreased slope, corresponding to the coefficient  $B$ .

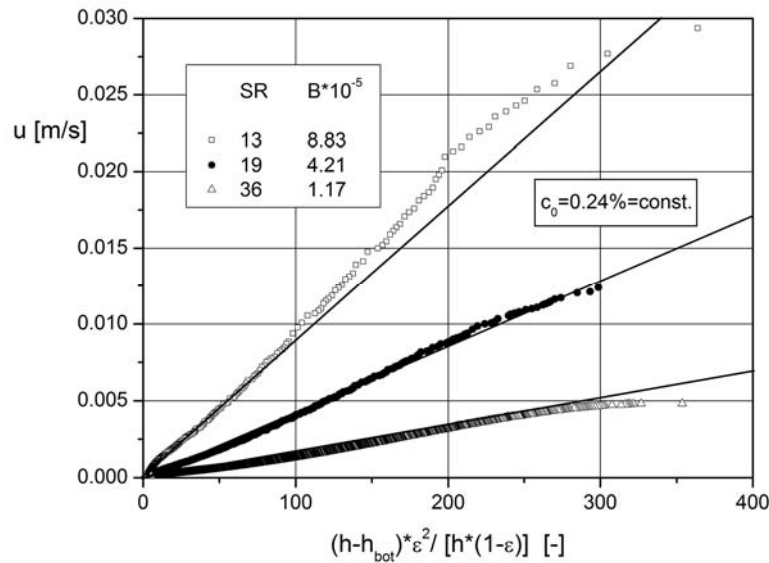


Fig. 7. Dependence of model parameters from pulp refining degree

Figure 7 proves that these considerations are valid. The higher the pulp refining degree (higher freeness value) the lower is the slope of the straight lines meaning lower velocities of the water flow. In the boundary case, for the pulp with values of 13°SR and 36°SR, the difference in the slope coefficients was 7.54. When expressed in terms of the average fibre diameter  $d_z$  it means a formal reduction of this dimension by 2.74 times.

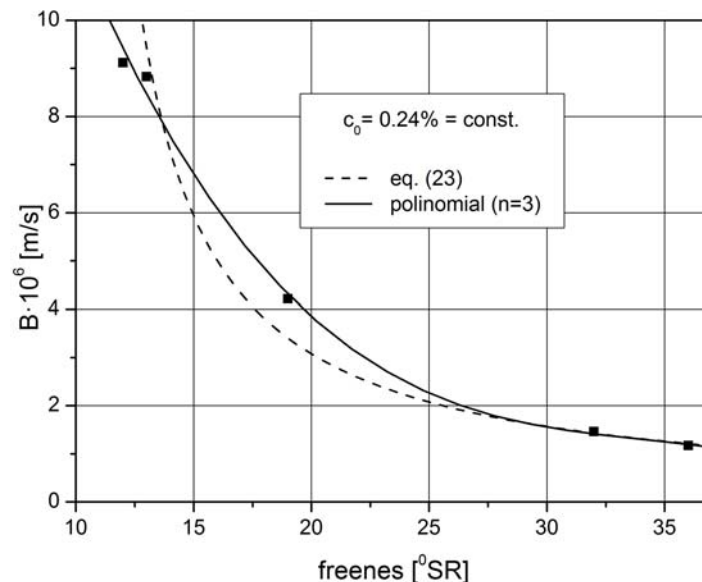


Fig. 8. Dependence of suspension drainage velocity from freeness value for concentration  $c_0=0.24\%$

Figure 8 shows a dependence of function  $B = f(^{\circ}SR)$ , where the value of  $B$  was determined in the same way as demonstrated in Fig. 7. The obtained relationship is not linear and its shape may suggest a hyperbolic function. Additionally, the lack of simple dependence of  $B$  on ( $^{\circ}SR$ ) may also result from a specific method of determining freeness.

The layout of the experimental points can be expressed by a polynomial of the third order (solid line) with the correlation coefficient  $R = 0.996$  and a displaced hyperbola of (23) with the correlation coefficient  $R = 0.991$ . Due to simplicity of the function (23) and a minor difference in the values of the correlation coefficients, Eq. (23) is recommended for further applications.

$$B = \frac{10^{-6}}{0.031 \cdot [SR] - 0.3} \text{ [m/s]} \quad (23)$$

Papermaking suspension contains a significant amount of fines (from 5% to even 50%), consisting of particles with a size below 0.2 mm. During technological processes, fines are partly removed from the suspension, but their impact on dewatering velocity should be significant during suspension drainage. Figure 9 confirms this assumption. For a suspension of 32°SR with no fines, the drainage velocity was five times higher than that with fines as assessed from the difference in values of the slope coefficients. It corresponds to an average diameter of the fibres that is about two and a half times higher for the pulp with removed fines. It is an obvious effect resulting from the removal of the smallest particles from the suspension.

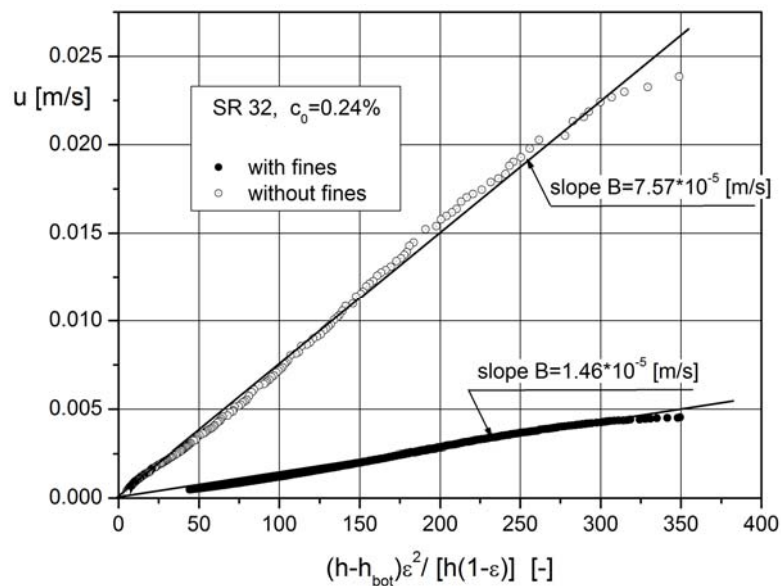


Fig. 9. Impact of the fines on suspension drainage velocity

## 5. CONCLUSIONS

- The results obtained from gravity drainage of the papermaking suspension do not validate the filtration and the capillary models describing the fluid flow through granular layers.
- The thickening mechanism is responsible for the velocity of gravity drainage on the paper machine wire.
- The velocity of gravity drainage can be estimated from a model proposed in this study (Eq. (11)). The proposed model was derived from the existing Ergun model.
- With a known difference between the pressures above and below the layer of suspension deposited on the wire in the papermaking machine, i.e. with the known driving force of drainage process and for the known suspension freeness value [°SR], we can calculate the drainage time from Eqs. (21) and (23).
- Equations (21) and (23) may be applicable for predicting the drainage rate. They can be also used to optimize the operation.

The authors gratefully acknowledge that this work was financially supported by the project LIDER/042/407/L-4/12/NCBR/2013 funded by National Center for Research and Development (Poland) and project no. W-10/1/2014/Dz. St.

## SYMBOLS

$A$	surface of cylinder bottom, $m^2$
$B$	constant in Eq. (21), $m/s$
$SR$	freeness, -
$V$	suspension volume that flowed through the bottom wire, $m^3$
$V_0$	initial suspension volume in the cylinder, $m^3$
$a_E$	constant in Eq. (6), -
$c_0$	initial pulp concentration, %
$d_z$	equivalent diameter of granule (fibre), $m$
$h$	actual height of liquid in the cylinder (suspension height), $m$
$h_{bot}$	flow resistance through the bottom, $m$
$k$	rate constant, $1/s$
$u$	velocity of liquid in the cylinder, $m/s$
$u_0$	real velocity of liquid during flow through suspension = $u/\varepsilon$ , $m/s$
$x$	mass (volume) fraction of liquid that flew through the bottom wire = $\frac{V}{V_0}$ , -

## Greek symbols

$\varepsilon$	porosity, -
$\eta$	dynamic viscosity, $Pa \cdot s$
$\lambda$	flow resistance coefficient, -
$\rho$	density, $kg/m^3$
$\varphi$	shape factor of single granule (fibre), -

## REFERENCES

- Blake F.C., 1922. The resistance of packing to fluid flow. *Trans. Am. Inst. Chem. Engrs.*, 14, 415-422.
- Britt K.W., Unbehend J.E. 1980. Water removal during sheet formation. *TAPPI*, 63, 4, 67.
- Britt K.W., Unberhend J.E., Shirdhran R, 1986. Observations on water removal in papermaking. *TAPPI*, 69, 7, 76.
- Carman P.C., 1937. Fluid flow through granular beds. *Trans. Inst. Chem. Eng.* 15, 150-166.
- Cole A.C., Hubbe M.A., Heitmann J.A., 2008. Water release from fractionated stock suspensions. Part 1-Effect of the amount and types of fibre fines. *TAPPI*, 28-31.
- Darby R., 1996. *Chemical Engineering Fluid Mechanics*, Marcel Dekker, Inc., 371-377.
- Ergun S., 1952. Flow through packed columns, *Chem. Eng. Prog.*, 48, 89-94.
- Hubbe M.A., Heitmann J.A., Cole C.A., 2008. Water release from fractionated stock suspensions. Part 2. Effects of consistency, flocculants, shear, and order of miting. *TAPPI*, August 14-19.
- Kozeny J., 1927. Über kapillare Leitung des Wassers im Boden (Aufstieg, Versickerung und Anwendung auf die Bewässerung), *Sber. Akad. Wiss., Wien*, 136 (Abt IIa) 271-306.
- Ortner G., 2001. Warum Altpapierfasern mahlen? *Wbl. Papierfabr.*, 129, 8, 483.
- Parker J.D., 1992. *The Sheet Forming Process*. TAPPI Special Technical Association Publication, Vancouver.
- Przybysz P., Kuncewicz C., Rieger F., 2014. A new device for characterisation of the drainage kinetics of fibrous suspensions under gravity. *Chem. Process Eng.*, 35, 409-420. DOI: 10.2478/cpe-2014-0031.
- Serwiński M., 1982. *Zasady inżynierii chemicznej i procesowej*, WNT Warszawa.

- Smook G.A., 1992. *Handbook for Pulp & Paper Technologists*. Angus Wild Publications, Vancouver.
- Wandelt P., Tarnawski W.Z., Perlińska-Sipa K., 2004. Upgrading corrugated base papers made of recycled fibres. *Proceedings of Pulp Paper Conference*, Helsinki, p. 169.
- Wandelt P., Tarnawski W.Z., Perlińska-Sipa K., 2005. Possibilities for upgrading OCC pulp by its refining and fines management. *Paperi Puu*, 87, 265.
- Wandelt P., Perlińska-Sipa K., 2007. Studies on the drainability of secondary pulps and the effect of fines content. *Przeląd Papierniczy*, 63, 547.
- Wandelt P., Perlińska-Sipa K., 2008. Possibilities of upgrading corrugated base paper made of OCC pulp without deterioration of its drainability. *Przeląd Papierniczy*, 64, 685.

*Received 08 September 2013*

*Received in revised form 08 July 2014*

*Accepted 24 July 2014*